

# High-strain piezoelectric ceramics and applications to actuators

Kazuaki Kurihara<sup>\*</sup>, Masao Kondo

*Fujitsu Ltd., 10-1 Morinosato-Wakamiya, Atsugi 243-0197, Japan*

Available online 2 October 2007

## Abstract

PZT-based solid solutions are very attractive piezoelectric ceramics, because they exhibit excellent piezoelectric properties such as large piezoelectric constant. In this paper we describe the relationship between piezoelectric properties and compositions, and sintering behavior of  $\text{PbNiNbTiO}_3\text{-PbTiO}_3\text{-PbZrO}_3$  (PNN–PT–PZ) ceramics and applications to the microactuators for magnetic disk drives. The MPB composition was determined by the temperature dependence of the relative permittivity and XRD patterns. The large piezoelectric constant ( $d_{33} = 1100$  pm/V) was obtained at the MPB composition. Unique rotating symmetrical microactuators using PNN–PT–PZ ceramics show both wide stroke and high-resonant frequency. In this paper we also describe the applications of piezoelectric ceramics to tunable superconductive filters for future wireless communication systems. Low-temperature piezoelectric properties of PZT-based ceramics and frequency tunable mechanisms will be discussed. This work was supported in part by the Ministry of Internal Affairs and Communications (MIC) of Japan.

© 2007 Elsevier Ltd and Techna Group S.r.l. All rights reserved.

*Keywords:* A. Sintering; C. Piezoelectric properties; D. PZT; E. Actuators

## 1. Introduction

Piezoelectric actuators are critical components in precision positioners, such as ultrasonic ac motors using resonating strain [1]. There are many designs for these ceramic actuator devices, though they all utilize the strain induced in the ceramic longitudinally or transversely to the applied electric field [2]. The multilayer actuator belongs to the first category (the strain is induced longitudinally) and is one of the typical designs for piezoelectric ceramic actuators. Single crystals of lead-containing perovskites have excellent piezoelectric constant ( $d_{33} = 1570$  pC/N) [3]. Those of piezoelectric ceramics, such as  $\text{Pb}(\text{Zr,Ti})\text{O}_3$  (hereafter PZT) and modified PZT, are smaller ( $d_{33}$  is around 650 pC/N) due to the grain boundary in the ceramic [4]. However, piezoelectric ceramics do have advantages. For example, they are applicable to large piezoelectric devices, and their preparation costs are much less than those of single crystals. What they lack is performance comparable to that of single crystals.

PZT ceramics are normally obtained by firing the green body of the powder at around 1250 °C [5]. This temperature is

slightly higher for multilayer applications co-fired with electrode materials. Decreasing the sintering temperature provides several advantages in the preparation of a multilayer device. For example, the composition of the internal electrode is an important factor in determining the manufacturing cost of a multilayer actuator. The melting point of the material of internal electrodes should be higher than the firing temperature, and the electrode material should have low reactivity with PbO in PZT ceramics. Therefore, platinum or silver–palladium alloys are commonly used for the internal electrodes. Another merit is the ability to control the ceramic composition. The vaporization of PbO decreases with decreasing temperature. Sol–gel processing is one of the effective methods utilized to decrease the sintering temperature of a powder [6]. However, it is difficult to prepare a large amount of powder by the sol–gel process, and the raw materials, such as organic metals, are more expensive than powders prepared by a solid–solution method.

The  $\text{Pb}(\text{Ni}_{1/3}\text{Nb}_{2/3})\text{O}_3\text{-PbTiO}_3\text{-PbZrO}_3$  (hereafter PNN–PT–PZ) ceramic is an attractive material for many piezoelectric applications because it has a large electromechanical-coupling coefficient for ceramics ( $k_{33} = 0.8$ ) [7–9]. Another feature of PNN–PT–PZ ceramics is that they can be sintered at relatively low temperatures. We have previously investigated the effect of excess lead oxide (PbO) on sintering behavior and on the surface microstructure of PNN–PT–PZ ceramics and found that

<sup>\*</sup> Corresponding author. Tel.: +81 46 250 8829; fax: +81 46 248 8812.

E-mail address: [kurihara.kazuak@jp.fujitsu.com](mailto:kurihara.kazuak@jp.fujitsu.com) (K. Kurihara).

ceramics with excess PbO could be liquid-phase sintered below 950 °C [10]. This firing temperature indicates that silver electrodes (melting point 962 °C) could be used as an internal electrode in a co-fired multilayer. We have already reported that the multilayer actuator made of PNN–PT–PZ ceramic with silver internal electrodes could be successfully fabricated by sintering at 900 °C [11,12].

Recently, the preparation of ceramics with compositional dependent on the piezoelectric constant in PNN–PT–PZ system with large longitudinal piezoelectric constant were investigated; along with the preparation and the basic reliability of the multilayer actuator with silver internal electrode.

## 2. Experimental procedure

First, the piezoelectric constant of ceramics with composition in the vicinity of morphotropic phase boundary (MPB) [9] was investigated. Fig. 1 showed the investigated composition area. The details of the preparation and evaluation of calcined PNN–PT–PZ powder are described elsewhere [9,10].

Multilayer actuators were prepared using the conventional tape-casting method. Pastes consisting of 100% silver powder (Ag) or coprecipitation powder of silver–30 mol% palladium (Ag–Pd) were used as internal electrode materials. The laminated green bodies were sintered at 900 °C in the sample with Ag internal electrode and at 1050 °C with Ag–Pd electrode for 6 h. The number of driving layers was 11, and each layer had a thickness of 36 μm.

The relative density was determined using the Archimedeian method. A value of 8.31 g/cm<sup>3</sup> for the theoretical density of the PNN–PT–PZ ceramic was derived from the lattice parameter and the composition. The microstructure of the fractured surface of the multilayer ceramic was observed with a field-emission-scanning electron microscope (FE-SEM, SH-100, Hitachi, Japan). The crystallinity of ceramics was determined by X-ray diffraction method (XRD, Rigaku, RAD-IIR, Japan). The piezoelectric constant was derived from the slope of the strain-electric field curve. The strain was measured using strain measurement apparatus (Toyoseiki, Japan). These measurements were taken using specimens sintered sufficiently at 1050 °C for 3 h. The capacitance, dielectric permittivity, and

resonance frequency were measured with an impedance analyzer (HP4194A, Hewlett-Packard). The piezoelectric constant was also calculated by resonant–antiresonant method. The displacement of the multilayer actuator was measured using the laser Doppler method. The details of evaluation procedure were described in the previous paper [11]. To evaluate reliability, the multilayer actuators were driven at 7.2 kHz for  $6 \times 10^{10}$  cycles in an environment of 40 °C and 90% humidity.

## 3. Results and discussion

Fig. 2 shows the change of piezoelectric constant ( $d_{33}$ ) of the ceramic with the composition of PNN–PT–PZ50/35/15 and 50/34/16 and  $2\theta$ – $\theta$  X-ray diffraction pattern measurement.

The (2 0 0)/(0 0 2) peaks of the XRD patterns of PNN–PT–PZ 50/35/15 and 50/34/16 showed tetragonal and rhombohedral phases, respectively. The open and closed circles in the map indicated the composition with the tetragonal and the rhombohedral peak patterns. Thus, this figure indicated that the MPB exists within these compositions. This area was identical with the MPB positions derived from electromechanical-coupling coefficient ( $k_{33}$ ) and dielectric permittivity ( $\epsilon_{33}^T/\epsilon_0$ ), as shown in a previous paper [9]. The  $d_{33}$  reached the maximum value at 915 pC/N of PNN–PT–PZ 50/34.5/15.5.

Fig. 3 shows the change of piezoelectric constant of the ceramic as a function of PT content (PNN = 50 mol%). Open circle plots were from the data measured by the resonant–antiresonant method at low electric fields less than 0.01 kV/cm, and closed circle plots were from the data of direct strain measurement using a strain meter at the high electric fields of about 10 kV/cm. The  $d_{33}$  calculated from the results of the resonant–antiresonant method was 915 pC/N for the PNN–PT–PZ 50/34.5/15.5, as shown in Fig. 2. The  $d_{33}$  derived from the strain measurement was 1100 pm/V for PNN–PT–PZ 50/34.5/15.5 [12]. This difference is due to the difference of driving voltage. In the strain measurement, the domain wall should move with an applied electric field, because the driving voltage

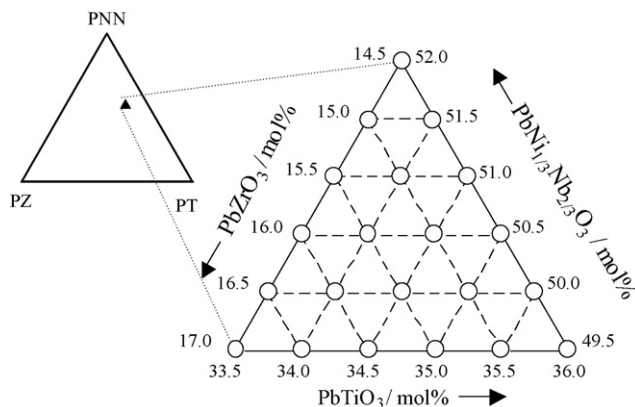


Fig. 1. Investigated composition area in this study.

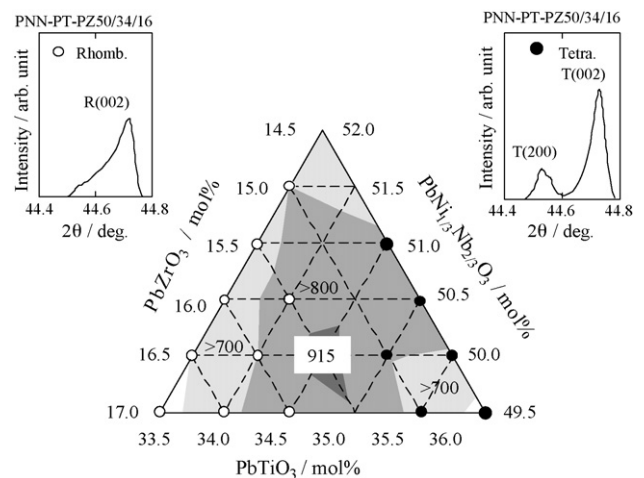


Fig. 2. Change in the piezoelectric constant ( $d_{33}$ ) and XRD patterns with the PNN–PT–PZ composition.

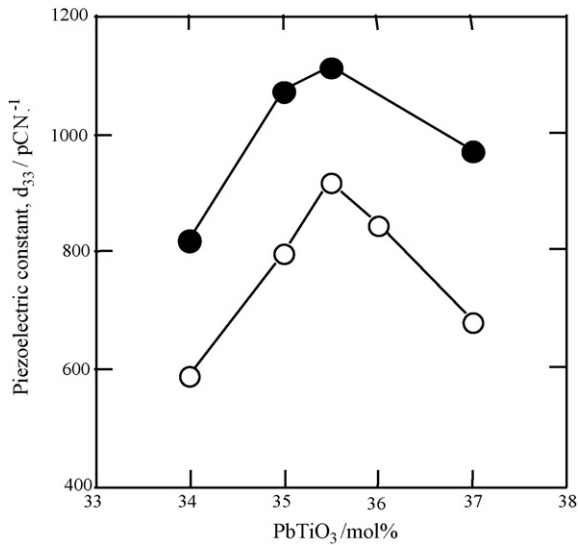


Fig. 3. Change in the piezoelectric constant ( $d_{33}$ ) derived from resonance and strain measurement (open circles) and direct strain measurement (closed circles) of PNN-PT-PZ ceramics.

is close to the coercive field (around 5 kV/cm). Thus, this difference is the contribution of the domain motion in the ceramics.

Fig. 4 shows the microstructures of the fractured surfaces of a multilayer actuator fabricated from PNN-PT-PZ ceramic with silver internal electrodes. The co-firing temperature was 900 °C. Since there were few pores between the grains, the ceramic–electrode interfaces did not have any de-lamination. The silver electrodes did not melt, and the multilayer ceramic was sufficiently densified at 900 °C. This work thus succeeded in developing a multilayer actuator with silver internal electrodes by using low-temperature sintering of PNN-PT-PZ ceramic. The displacement of the multilayer actuator with Ag internal electrode was similar to those obtained from Ag-Pd electrode and had already been reported in the previous work [11].

Fig. 5 showed the results of the long-term change in the displacements of the multilayer actuators with Ag electrodes and Ag-Pd electrodes. The co-firing temperatures of multilayer

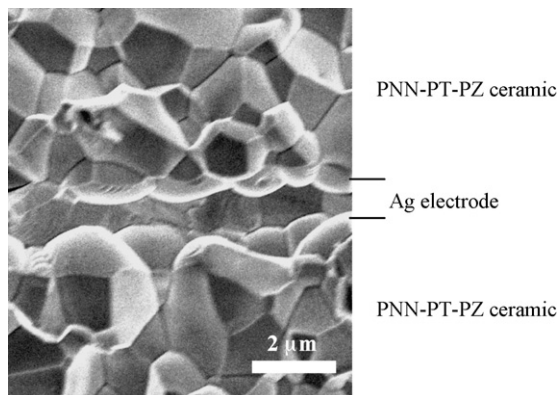


Fig. 4. Microstructure of the fractured surface of multilayer actuator co-fired with Ag electrodes at 900 °C.

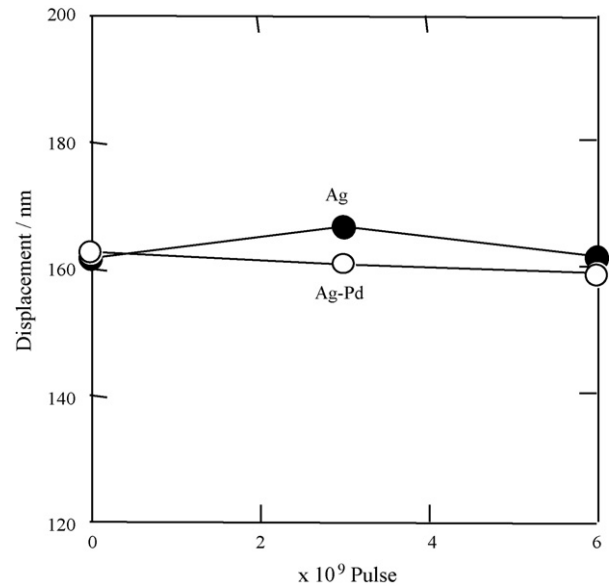


Fig. 5. The long-term change in the displacements of multilayer actuators with Ag electrodes and Ag-Pd electrodes. The sintering temperatures of Ag and Ag-Pd electrodes samples were 900 °C and 1050 °C, respectively.

actuators with Ag and Ag-Pd electrodes were 900 °C and 1050 °C, respectively. These actuators were driven with an ac bias at 7.2 kHz, in the controlled environment with humidity of 90% and a temperature of 40 °C. The displacements of both actuators did not change even after  $6 \times 10^{10}$  pulses. High performance and reliability of the multilayer actuators can thus be fabricated using PNN-PT-PZ ceramic and silver internal electrodes.

#### 4. Application to HDD microactuators

In recent years, the aerial density of the magnetic disk drive has increased by 70–100% every year, mainly based on the improvement of recording heads and media. There has been an increasing demand of wider servo band to achieve stable operation at a higher track density. However, the servo bandwidth of voice-coil motor (VCM) systems, which are widely used for positioning the magnetic head, is limited by the mechanical resonances of the carriage, coil, and suspension. One possible solution to achieve a higher track density is the dual-stage actuator system using a piezoelectric microactuator which drives the head slider directory.

Fig. 6 shows a schematic structure of the author's new piezoelectric microactuator system [13]. Two piezoelectric multilayer actuators made of PNN-PT-PZ ceramics are placed between a head slider and a suspension. The actuators are bonded diagonally to a slider and suspension. The unique feature of the actuator system is a symmetrical structure. Because of conformation of a center of gravity and an axis of rotation, excitation of a resonance of the suspension will be minimized. This is an important concept of the new actuator system. Another feature of the actuator system is a very simple structure, especially using simple-shaped piezoelectric actuator elements which are the same as widely used rectangular-shaped ones.

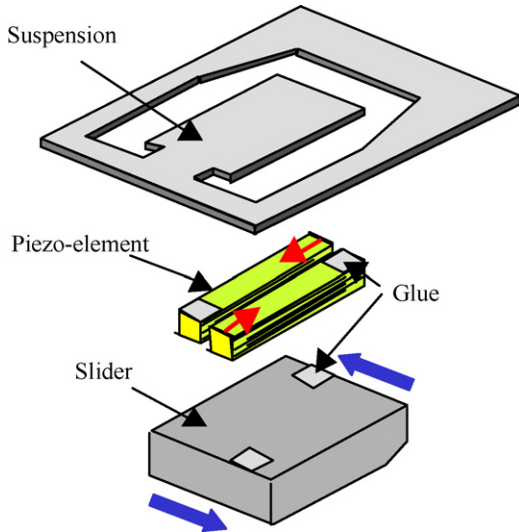


Fig. 6. Schematic structure of system.

In this study, design targets are wide slider moving stroke of  $1\ \mu\text{m}$  at 30 V operation and high-resonance frequency over 20 kHz for wider servo bandwidth. FEM analysis was performed in order to get a suitable design which covers the design specifications. The model used in this study is whole HGA consisting of 30% pico-slider, two piezoelectric microactuator elements and suspension. The suspension also consists of a gimbal and loadbeam. The air springs were also taken into account because the slider was flying above a rotating disk. The detailed design was fixed by comparing the results of static analysis, modal analysis, and frequency response analysis.

Fig. 7 shows the result of displacement distribution by FEM analysis of the HGA. The displacement of the head element is  $0.93\ \mu\text{m}$  at an applied voltage of 30 V. This is very close to our displacement target of  $1\ \mu\text{m}$  at 30 V applied.

Fig. 8 shows a simulation result of the frequency response. The main resonance frequency of the actuator is 26.3 kHz, which is higher than the expected target of 20 kHz. Note that the excitation of the suspension near 14 kHz is very small compared to that of the actuator. The reason for this small resonance is a unique feature of the symmetrical actuator structure.

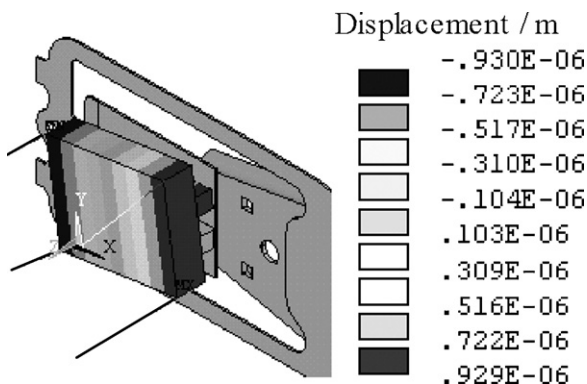


Fig. 7. FEM simulation result of microactuator displacement distribution.

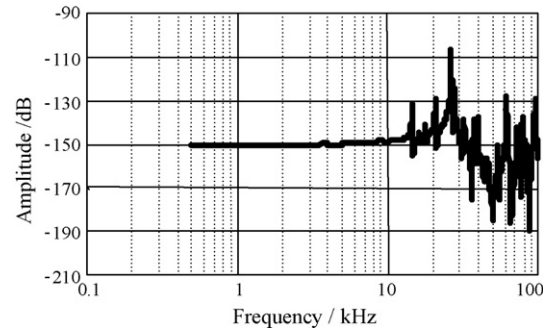


Fig. 8. Calculated frequency response.

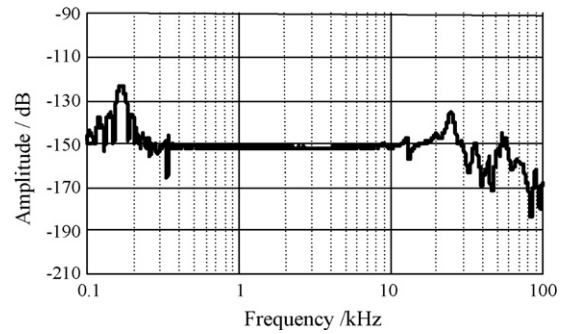


Fig. 9. Measured frequency response.

The measured displacement at the head edges (head element side and carriage side) at an applied voltage of 30 V was  $0.91\ \mu\text{m}$  and  $0.89\ \mu\text{m}$ , respectively. Those are very close to calculated value of  $0.93\ \mu\text{m}$ . Fig. 9 shows the measured frequency response of the fabricated HGA using a piezoelectric microactuator. The resonance frequency of the actuator is 25.1 kHz. This is also very close to the calculated values. Measured peaks near 14 kHz, which are the excitation of the suspension, are very small compared to the resonance of actuator.

### 5. Application to tunable superconducting filters

Effective use of frequency resources is very important for future wireless communication. In the future system, dynamic

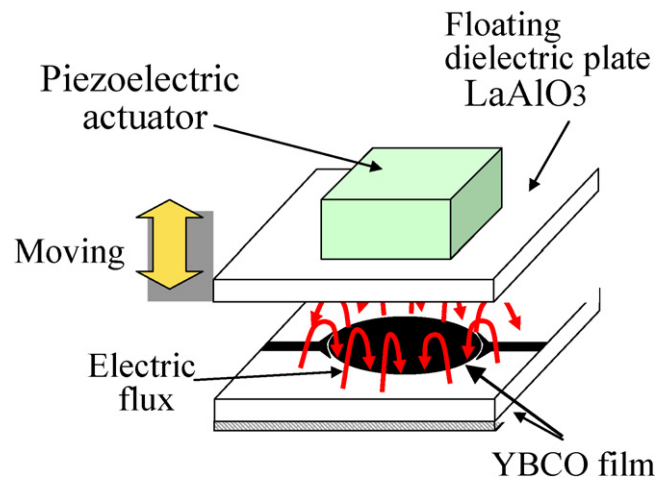


Fig. 10. Model of a candidate of tunable superconducting resonator.



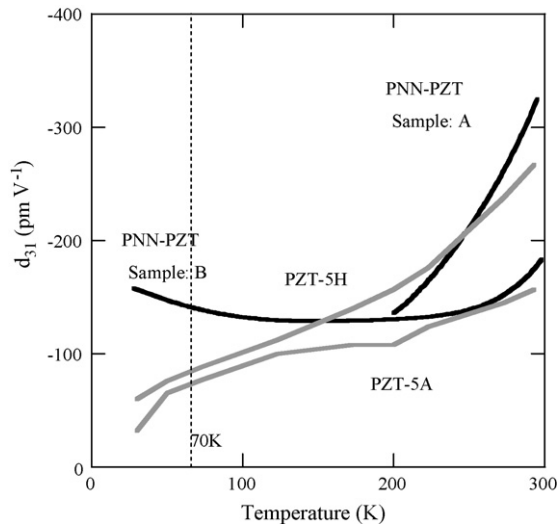


Fig. 11. Low-temperature piezoelectric properties.

frequency transmission with a steep filter profile is required. Tunable superconducting filters are very useful devices for the system because of its very steep and low loss profiles owing to very high- $Q$  factors of the superconductors. Fig. 10 shows a method of tuning the resonant frequency of superconducting filters. A disc shape pattern of hetero-epitaxial YBCO thin films was formed on an MgO single crystal substrate as a resonator. Resonant frequency of the structure can be tuned by changing the distance between the substrate and the floating dielectric plate. Piezoelectric actuators are the best selection to move the dielectric plate with fast and fine adjustment, but must be used at 70 K. Usually, properties of piezoelectric ceramics decrease with lowering temperature. New materials are therefore required for low-temperature operations. Fig. 11 shows the low temperature properties of the piezoelectric ceramics. PZT-5A, PZT-5H and PNN–PTZ sample A, which are near the MPB composition, showed a decrease of the  $d_{31}$  value with lowering temperature. MPB composition PNN–PZT sample A showed a high  $d_{31}$  value at room temperature but decrease rapidly with lowering of the temperature. On the other hand, PNN–PZT sample B, which was not a MPB composition, showed negative temperature dependence below 150 K and at 70 K, which is the operating temperature of the superconductive filters, and is considered a very high value as compared to PZT ceramics. This ceramic composition may be very useful for superconductive applications.

## 6. Conclusions

The piezoelectric properties and sinterability of  $\text{Pb}(\text{Ni}_{1/3}\text{Nb}_{2/3}\text{O}_3\text{--PbTiO}_3\text{--PbZrO}_3)$  (PNN–PT–PZ) ceramics for actuator application were investigated. Compositions near MPB strongly affected piezoelectric properties. A ceramic with a

large piezoelectric constant ( $d_{33} = 1100 \text{ pm/V}$ ) was obtained on the MPB composition of PNN–PT–PZ 50/34.5/15.5.

Piezoelectric microactuator systems for HDD were fabricated using PNN–PT–PZ ceramics. Results of FEM analysis and measured data of fabricated HGA are in good agreement and show large displacements and excellent vibration characteristics.

PNN–PT–PZ ceramics having good low temperature properties for superconductive applications were obtained.

## Acknowledgement

This work was supported in part by contract research “Research and development of fundamental technologies for advanced radio frequency spectrum sharing in mobile communication systems” from the Ministry of Internal Affairs and Communications (MIC) of Japan.

## References

- [1] K. Uchino, The trend of micro-mechatronics and piezoelectric/electrostrictive actuators, in: H.L. Tuller (Ed.), *Piezoelectric Actuators and Ultrasonic Motors*, 2nd ed., Kluwer Academic Publishers, Boston, 1997, pp. 1–12.
- [2] K. Uchino, Structures and fabrication process of ceramic actuators, in: H.L. Tuller (Ed.), *Piezoelectric Actuators and Ultrasonic Motors*, 2nd ed., Kluwer Academic Publishers, Boston, 1997, pp. 121–1256.
- [3] J. Kuwata, K. Uchino, S. Nomura, Dielectric and piezoelectric properties of  $0.91\text{Pb}(\text{Zn}_{1/3}\text{Nb}_{2/3}\text{O}_3\text{--}0.09\text{PbTiO}_3)$  single crystals, *Jpn. J. Appl. Phys.* 21 (1982) 1298–1302.
- [4] Y. Yamashita, Large electromechanical coupling factors in perovskite binary material system, *Jpn. J. Appl. Phys.* 33 (9B) (1994) 5328–5331.
- [5] D.A. Buckner, P.D. Wilcox, Effects of calcining on sintering of lead zirconate–titanate ceramics, *Ceram. Bull.* 51 (3) (1972) 218–222.
- [6] P. Duran, C. Moure, Sintering at near theoretical density and properties of PZT ceramics chemically prepared, *J. Mater. Sci.* 20 (1985) 827–833.
- [7] M. Kondo, M. Hida, M. Tsukada, K. Kurihara, N. Kamehara, Piezoelectric properties of  $\text{PbNi}_{1/3}\text{Nb}_{2/3}\text{O}_3\text{--PbTiO}_3\text{--PbZrO}_3$  ceramics near the MPB, *J. Ceram. Soc. Jpn.* 105 (8) (1997) 719–721.
- [8] M. Kondo, M. Hida, M. Tsukada, K. Kurihara, N. Kamehara, Piezoelectric properties of  $\text{PbNi}_{1/3}\text{Nb}_{2/3}\text{O}_3\text{--PbTiO}_3\text{--PbZrO}_3$  ceramics, *Jpn. J. Appl. Phys.* 36 (9B) (1998) 6043–6045.
- [9] M. Kondo, M. Hida, M. Tsukada, K. Kurihara, M. Kutami, N. Kamehara, Piezoelectric properties and phase transitions of  $\text{PbNi}_{1/3}\text{Nb}_{2/3}\text{O}_3\text{--PbTiO}_3\text{--PbZrO}_3$  ceramics, in: E. Colla, D. Damjanovic, N. Setter (Eds.), *Proceedings of the 11th IEEE International Symposium on the Applications of Ferroelectrics, IEEE Ultrasonic, Ferroelectrics and Frequency Control Society*, New Jersey, 1998, pp. 311–314.
- [10] M. Kondo, K. Kurihara, Sintering behavior and surface microstructure of PbO-rich  $\text{PbNi}_{1/3}\text{Nb}_{2/3}\text{O}_3\text{--PbTiO}_3\text{--PbZrO}_3$  ceramics, *J. Am. Ceram. Soc.* 84 (2001) 2469–2474.
- [11] M. Kondo, K. Kurihara, Preparation of  $\text{PbNi}_{1/3}\text{Nb}_{2/3}\text{O}_3\text{--PbTiO}_3\text{--PbZrO}_3$  ceramic multilayer actuator with silver internal electrodes, *Sensor Actuator A* 109 (2003) 143–148.
- [12] M. Kondo, K. Kurihara, Piezoelectric properties and applications of  $\text{PbNi}_{1/3}\text{Nb}_{2/3}\text{O}_3\text{--PbTiO}_3\text{--PbZrO}_3$  ceramics, *Key Eng. Mater.* (2003) 230–231.
- [13] T. Mita, K. Kurihara, M. Hida, S. Koganezawa, Abstract of Spring Meeting of Jpn. Soc. for Precision Eng., Jpn. Soc. for Precision Eng., Tokyo, Japan, 2002, 115 pp..